Biophysical Chemistry 148 (2010) 121–130

Contents lists available at ScienceDirect

Biophysical Chemistry

journal homepage: http://www.elsevier.com/locate/biophyschem

Thermal stability and aggregation of creatine kinase from rabbit skeletal muscle. Effect of 2-hydroxypropyl-β-cyclodextrin

Olga I. Maloletkina [a], Kira A. Markossian [a], Lyubov V. Belousova [b], Sergey Yu Kleimenov [a], Victor N. Orlov [c,d], Valentina F. Makeeva [a], Boris I. Kurganov [a,*]

[a] Bach Institute of Biochemistry, Russian Academy of Sciences, Moscow, Russia
[b] Department of Biochemistry, Faculty of Biology, Lomonosov Moscow State University, Moscow, Russia
[c] Belozersky Institute of Physico-Chemical Biology, Moscow State University, Moscow, Russia
[d] Faculty of Bioengineering and Bioinformatics, Moscow State University, Moscow, Russia

ARTICLE INFO

Article history:
Received 28 December 2009
Received in revised form 3 March 2010
Accepted 5 March 2010
Available online 16 March 2010

Keywords:
Creatine kinase
2-Hydroxypropyl-β-cyclodextrin
Inactivation
Denaturation
Aggregation

ABSTRACT

Effect of 2-hydroxypropyl-β-cyclodextrin (HP-β-CD) on thermal aggregation of creatine kinase from rabbit skeletal muscle (RMCK) at 48 °C has been studied using dynamic light scattering. An increase in the duration of the lag period on the kinetic curves of aggregation, registered as an increment of the light scattering intensity in time, has been observed in the presence of HP-β-CD. It has been shown that the initial parts of the dependences of the hydrodynamic radius (R_h) of the protein aggregates on time follow the exponential law. The reciprocal value of parameter t_{2R} (t_{2R} is the time interval over which the R_h value is doubled) was used to characterize the rate of aggregation. A 10-fold decrease in the $1/t_{2R}$ value was observed in the presence of 76 mM HP-β-CD. Judging from the data on the kinetics of RMCK inactivation and the data on differential scanning calorimetry of RMCK, HP-β-CD does not affect the rate of RMCK unfolding.

1. Introduction

Cyclodextrins (CDs) are cyclic oligosaccharides obtained by the enzymatic conversion of starch [1]. The natural CDs – α-, β- and γ-CD – contain six, seven or eight glucopyranose units, respectively, linked through α-1,4 glycosidic bonds [2]. Since natural CDs have a relatively low solubility in aqueous solutions, a variety of CD derivatives with enhanced aqueous solubility have been developed. Some synthetic derivatives, such as hydroxypropyl-β-cyclodextrin (HP-β-CD), show higher solubility in water [1,3]. If solubility of β-CD in water at 25 °C is 18.5 mg mL^{-1}, then that of HP-β-CD is higher than 600 mg mL^{-1}.

CDs have a rigid conical molecular structure with a hydrophobic interior and a hydrophilic exterior [4]. The internal cavity can include a wide range of guest molecules, ranging from polar compounds such as alcohols, acids, amines and small inorganic anions to apolar compounds such as aliphatic and aromatic hydrocarbons. In turn, the hydrophilic exterior facilitates solution of CDs in water [5]. As a result CDs can interact with appropriately sized hydrophobic molecules in aqueous environment and form host–guest inclusion complexes [6]. Formation of the inclusion complexes of CDs with guest molecules is due to non-covalent interactions and steric factors [7]. Each CD has its own ability to form inclusion complexes with specific guests, and this ability depends on a suitable fit of the guest molecule into the hydrophobic CD cavity [3,8,9]. The ability of CDs to form the inclusion complexes is very important in the pharmaceutic industry, in terms of drug solubility, stability and bioavailability.

CDs are able to form host–guest inclusion complexes with the accessible hydrophobic side chains of amino acids in proteins and peptides and can affect their stability. According to the data on differential scanning calorimetry (DSC), circular dichroism and intrinsic protein fluorescence, α-CD, γ-CD and 6-O-α-D-glucosyl-β-CD provoke the decrease in the thermal stability of hen and chicken egg white lysozyme [10,11] and bovine pancreatic ribonuclease A [12]. α-CD causes the decrease in the thermal stability of ubiquitin, yeast phosphoglycerate kinase [10]. It has been shown that HP-β-CD accelerates thermal inactivation and decreases the thermal stability of rabbit muscle glyceraldehyde-3-phosphate dehydrogenase (GAPDH) [13].

Studies of the effect of various CDs on protein aggregation have demonstrated an ability of CDs to inhibit protein aggregation. For example, the ability of α-CD to suppress thermal aggregation of horse liver alcohol dehydrogenase has been revealed [14]. The study of the influence of β-CD and various β-CD derivatives on protein aggregation at elevated temperature demonstrated that β-

Abbreviations: CD, cyclodextrin; DLCA, diffusion-limited cluster–cluster aggregation; DLS, dynamic light scattering; DSC, differential scanning calorimetry; HP-β-CD, hydroxypropyl-β-cyclodextrin; RLCA, reaction-limited cluster–cluster aggregation; RMCK, rabbit muscle creatine kinase.

* Corresponding author. Tel.: +7 495 952 5641; fax: +7 495 954 2732.
E-mail address: kurganov@inbi.ras.ru (B.I. Kurganov).

0301-4622/$ – see front matter © 2010 Elsevier B.V. All rights reserved.
doi:10.1016/j.bpc.2010.03.005

CD was able to inhibit aggregation of α-amylase [15], indole–β-CD was found to be able to prevent aggregation of citrate synthase [16] and HP-β-CD as well as methylated β-CD suppressed thermal aggregation of salmon polypeptide calcitonin [17]. The ability of α-, β- and γ-CDs, as well as several hydroxypropyl and sulfobutyl ether cyclodextrins of varying degrees of substitution, to suppress thermally induced aggregation of three proteins (Clostridium difficile Toxoid A, *Yersinia pestis* low-calcium-response V or V antigen and fibroblast growth factor 10) was demonstrated by Samra et al. [18]. This study suggested that the stabilization of proteins by cyclodextrins was dictated by their type and degree of substitution, as well as the physical and chemical properties of the protein being examined. It is of interest, that in the case of natively unfolded proteins, such as beta-amyloid, the relatively low concentrations of HP-β-CD can promote aggregation to oligomeric and fibrillar aggregates as demonstrated by Wang et al. [19].

Creatine kinase (CK; ATP: creatine N-phosphotransferase, EC 2.7.3.2) is a key enzyme of cellular energy metabolism, catalyzing the reversible transfer of the high-energy phosphate group from ATP to creatine. Cytosolic CK from rabbit muscle (RMCK) is a dimer consisting of two identical subunits of 380 residues, each with a molecular weight of 43 kDa [20]. The crystal structure of RMCK shows that each subunit has a limited number of contacts with residues in other subunits, including eight hydrogen bonds and a few water-mediated interactions at the dimer interface [21]. The RMCK monomer consists of two domains: a smaller N-terminal domain, containing only α-helices, and a larger C-terminal domain, containing an anti-parallel β-sheet surrounded by several long α-helices. The long loop in the N-terminal domain (from residue N63 to S81) is involved in the intra-subunit domain–domain interactions [22]. N-terminal and C-terminal domains are connected by a long linker, and the active site of the enzyme is located in the cleft between two domains [22]. Conformational change in the C-terminal domain is responsible for the initiation of CK thermal aggregation [23].

Studies of RMCK thermal denaturation and aggregation are few in number [24–29]. A fast loss in RMCK activity was observed at a temperature below the T_{max} (56 °C) on the DSC profile [25,30].

It has been shown that the thermal inactivation of CK is due to the conformational changes of its active sites [23,25]. Minor conformational changes in the active site and C-terminal domain might result in the modification of the domain–domain interactions and the formation of an inactive dimeric form which is prone to aggregate. The changes in domain–domain interactions may play a crucial role in thermal denaturation and aggregation of RMCK [23].

In the present study we investigated the effect of HP-β-CD on thermal inactivation, denaturation and aggregation of RMCK. The increment of the light scattering intensity and the growth of the protein aggregates in the course of RMCK aggregation were registered by dynamic light scattering (DLS). The analysis of the dependences of the light scattering intensity and the hydrodynamic radius of the protein aggregates on time allowed obtaining the quantitative characteristics of the aggregation process. These quantitative characteristics were used to describe the suppression of RMCK aggregation by HP-β-CD. The results of the study of the action of HP-β-CD on the kinetics of thermal inactivation and denaturation of RMCK showed that HP-β-CD did not affect the rate of RMCK unfolding.

2. Materials and methods

2.1. Materials

2-Hydroxypropyl-β-cyclodextrin (HP-β-CD, degree of substitution 3 ± 1, water content less than 5%, CY-2005.1, batch number CYL-2278) was purchased from CycloLab (Hungary). RMCK, Hepes, NaCl and lyophilized salt-free RMCK were purchased from Sigma (USA). All solutions for the experiments were prepared using de-ionized water obtained with Easy-Pure II RF system (Barnstead, USA). RMCK concentration was determined spectrophotometrically at 280 nm with the extinction coefficient $A^{1\%}_{1\,cm}$ of 8.8 [31].

2.2. Determination of refractive index, density and dynamic viscosity of HP-β-CD solutions

The values of the refractive index of the HP-β-CD solutions in 30 mM Hepes–NaOH buffer, pH 8.0, 0.1 M NaCl, were determined in refractometer IRF-22 (Russia) at 48 °C (Table 1). Based on the obtained data the refractive index increment was estimated: $dn/dc = 0.169 \pm 0.001\ M^{-1}$.

Density of HP-β-CD solutions at concentrations of 0–76 mM in 30 mM Hepes–NaOH buffer, pH 8.0, 0.1 M NaCl was determined in density meter DMA 4500 "Anton Paar" (Austria). Dynamic viscosity of 30 mM Hepes–NaOH buffer, pH 8.0, 0.1 M NaCl in the presence of different HP-β-CD concentrations (0–76 mM) was determined in automatic microviscosimeter "Anton Paar" (Austria) in system 1.6/1.500 mm at 48 °C. The obtained values of density and dynamic viscosity are given in Table 1.

The partial specific volume of HP-β-CD was calculated from the expression: $\rho = \rho_0 + (1 - \bar{v}\rho_0)c$, where ρ and ρ_0 are the densities of solution and solvent, respectively, c is the concentration of HP-β-CD and $\bar{v}$ is the partial specific volume (see [32]). The value of $\bar{v}$ was found to be $0.700 \pm 0.002\ cm^3\ g^{-1}$.

The values of refractive index and dynamic viscosity of HP-β-CD solutions were used in the DLS measurements.

2.3. Assay of RMCK

RMCK enzymatic activity was estimated according to the potentiometric method [33]. The kinetics of the reaction was registered at 30 °C in 10 mM Tris–HCl, pH 7.6, containing 10 mM KCl and 6 mM Mg $(CH_3COO)_2$. The reaction mixture contained 5 mM creatine phosphate and 1 mM ADP. The reaction was initiated by the addition of the enzyme to the reaction mixture. The final preparations usually had a specific activity of 220–250 μmol min^{-1} mg^{-1}. The relative error in the estimation of the enzymatic activity was 3%.

2.4. Thermal inactivation of RMCK

The kinetics of thermal inactivation of RMCK was studied by incubating the enzyme solutions in the absence or in the presence of various concentrations of HP-β-CD in 30 mM Hepes–NaOH buffer, pH 8.0, 0.1 M NaCl at 48 °C. Heated samples were removed at suitable time intervals and immediately cooled down to 30 °C in the ice water bath. Aliquots were withdrawn from heated samples and added to the reaction mixture to determine the enzymatic activity at 30 °C.

2.5. Calorimetric studies

Thermal denaturation of RMCK in 30 mM Hepes–NaOH buffer, pH 8.0, 0.1 M NaCl, was studied by DSC. DSC experiments were performed using a DASM-4 M differential scanning microcalorimeter (Institute

Table 1
Refractive index (n), density (ρ) and dynamic viscosity (η) of HP-β-CD solutions at 48 °C (30 mM Hepes–NaOH buffer, pH 8.0, 0.1 M NaCl).

[HP-β-CD], mM	n	ρ, g/cm^3	η, mPa s
0	1.3345 ± 0.0002	0.99803 ± 0.00005	0.6109 ± 0.0003
4	1.3350 ± 0.0002	0.99943 ± 0.00005	0.6214 ± 0.0002
8	1.3358 ± 0.0002	1.00149 ± 0.00005	0.6298 ± 0.0002
15	1.3370 ± 0.0002	1.00419 ± 0.00005	0.6423 ± 0.0003
38	1.3410 ± 0.0002	1.01310 ± 0.00005	0.6952 ± 0.0002
61	1.3448 ± 0.0002	–	–
76	1.3473 ± 0.0002	1.02814 ± 0.00005	0.8097 ± 0.0003

for Biological Instrumentation, Pushchino, Russia). Protein solutions were heated at a constant rate of 1 °C min^{-1} from 5 to 90 °C and at a constant pressure of 2.2 atm. The irreversibility of the thermal transition of RMCK was proved by checking the reproducibility of the calorimetric trace in a second heating of the sample immediately after cooling. Calorimetric traces of irreversibly denaturing protein were corrected for instrumental background and for possible aggregation artifacts by subtracting the scans obtained from the second heating of the samples. The temperature dependences of the excess heat capacity were further analyzed and plotted using Origin software (MicroCal Inc., USA).

2.6. Determination of the portion of aggregated RMCK

Samples of RMCK or mixtures of RMCK with HP-β-CD were incubated in microcentrifuge tubes at 48 °C in the solid state thermostat ThermoHAAKE DC-10 (Germany) in 30 mM Hepes–NaOH buffer, pH 8.0, 0.1 M NaCl. Each tube was removed after an appropriate time interval, immediately placed in the ice water bath and then centrifuged for 30 min at 20,000 ×*g*. The optical density (OD) of supernatant was measured at 280 nm. The portion of the aggregated protein (γ_{agg}) was calculated as $(1-OD/OD_0)$, where OD_0 is the optical density of the unheated solution.

2.7. Fluorescence measurements

Fluorescence spectra were recorded on Cary Eclipse spectrofluorometer (Varian, USA). All measurements were carried out at 20 °C. Tryptophan fluorescence was excited at 297 nm with 5 nm bandwidth for both excitation and emission slits, and emission was detected in the interval from 305 to 395 nm. When registering the fluorescence spectra of RMCK solutions preincubating at 48 °C for various time intervals, the aggregated protein was removed as described in the previous section. Since the concentrations of RMCK in heated samples were different, obtained spectra were normalized by amplitude.

2.8. Dynamic light scattering studies

Light scattering measurements were performed on a commercial instrument Photocor Complex (Photocor Instruments Inc., USA; www.photocor.com), as described earlier [34–36]. A He–Ne laser (Coherent, USA, Model 31-2082, 632.8 nm, 10 mW) was used as the light source. The temperature of sample cell was controlled by the proportional integral derivative temperature controller to within ±0.1 °C. A quasi-cross correlation photon counting system with two photomultiplier tubes was used to increase the accuracy of particle sizing in the range from 0.5 nm to 5.0 μm. DLS data have been accumulated and analyzed with multifunctional real-time correlator Photocor-FC. DynaLS software (Alango, Israel) was used for polydispersity analysis of DLS data.

The diffusion coefficient D of the particles is directly related to the decay rate τ_c of the time-dependent correlation function for the light-scattering intensity fluctuations: $D=1/2\tau_c k^2$. In this equation k is the wave number of the scattered light, $k=(4\pi n/\lambda)\sin(\theta/2)$, where n is the refractive index of the solvent, λ is the wavelength of the incident light in vacuum and θ is the scattering angle. The mean hydrodynamic radius of the particles, R_h, was calculated according to the Stokes–Einstein equation: $D=k_BT/6\pi\eta R_h$, where k_B is Boltzmann's constant, T is the absolute temperature and η is viscosity of the solution.

Thermal aggregation of RMCK was studied in 30 mM Hepes–NaOH buffer, pH 8.0, 0.1 M NaCl. The buffer was placed in a cylindrical cell with a diameter of 6.3 mm and preincubated for 5 min at an appropriate temperature. For incubation at a high temperature cells with stoppers were used to avoid evaporation. The aggregation process was initiated by the addition of an aliquot of RMCK to a final volume of 0.4 mL. To study the effect of HP-β-CD on RMCK aggregation at 48 °C, HP-β-CD was preincubated with buffer in the cell for 5 min before addition of an aliquot of RMCK. The scattering light was collected at 90° scattering angle.

Our studies of thermal aggregation of proteins by DLS have shown that the first stage of the aggregation process is the formation of the start aggregates including hundreds of denatured protein molecules [37]. Further sticking of the start aggregates and aggregates of higher order proceeds in the regime of diffusion-limited cluster–cluster aggregation (DLCA). When this regime is fulfilled, the sticking probability for the colliding particles is equal to unity. For aggregation that proceeds in the DLCA regime the initial part of the dependence of the hydrodynamic radius (R_h) of protein aggregates on time is linear. Above a definite point of time ($t=t^*$) the dependence of R_h on time follows the power law [34,38]:

$$R_h = R_h^*\left[1 + K_1(t-t^*)\right]^{1/d_f}, \quad (1)$$

where R_h^* is the R_h value at $t=t^*$, K_1 is a constant and d_f is the fractal dimension of the aggregates. When aggregation of colloidal particles proceeds in the DLCA regime, a universal fractal dimension (d_f) of 1.8 is observed [39,40].

The deceleration of the aggregation rate results in the transition of the aggregation process from the DLCA regime to the regime of the reaction-limited cluster–cluster aggregation (RLCA), wherein the sticking probability for the colliding particles becomes lower than unity. For aggregation of colloidal particles proceeding in the RLCA regime the initial part of the dependences of the hydrodynamic radius of aggregates on time follows the exponential law [39]. In the case of thermal aggregation of proteins the RLCA regime is observed when the protein substrate in itself reveals the chaperone-like activity (as with yeast alcohol dehydrogenase [41]) or aggregation is studied in the presence of a chaperone (for example, in the presence of α-crystallin) [34,35,42–47].

Given that the initial stage of thermal aggregation of proteins is the stage of formation of the start aggregates, we can write the following equation for the dependence of the hydrodynamic radius of the protein aggregates on time for the aggregation process proceeding in the RLCA regime:

$$R_h = R_{h,0}\exp\left[\frac{\ln 2}{t_{2R}}(t-t_0)\right], \quad (2)$$

where $R_{h,0}$ is the hydrodynamic radius of the start aggregates, t_0 is the moment of time at which the start aggregates come to view and t_{2R} is the time interval over which the hydrodynamic radius is doubled. The value of $1/t_{2R}$ characterizes the rate of aggregation (the higher the $1/t_{2R}$ value, the higher is the rate of aggregation).

2.9. Calculations

Origin 8.0 (OriginLab Corporation, USA) software and Scientist (MicroMath, Inc., USA) software were used for the calculations. To characterize the degree of agreement between the experimental data and calculated values, we used the coefficient of determination R^2 [48].

3. Results and discussion

3.1. Effect of HP-β-CD on thermal inactivation of RMCK

The effect of HP-β-CD on thermal inactivation of RMCK (0.2 mg mL^{-1}) was studied at 48 °C. The shape of the kinetic curve of inactivation indicates that the inactivation process consists of two stages (Fig. 1). Such a shape of the inactivation curve agrees with the results obtained by Bai et al. [25], who studied the kinetics of thermal inactivation of RMCK at 50 °C.

The following simplest model may be proposed for the quantitative description of the kinetics of inactivation:

$$\underset{a_N}{N} \xrightarrow{k_{tr}} \underset{a_{N^*}}{N^*} \xrightarrow{k_d} D. \quad (3)$$

In this model N is the native state of the enzyme, N^* is the conformationally changed state that retains, in part, the enzymatic activity, D is the denatured state that is catalytically inactive, k_{tr} is the rate constant for the conformational transition $N \rightarrow N^*$ and k_d is the rate constant for protein unfolding. If this model is valid, the decline of the relative enzymatic activity in time is described by the following equation, which is a sum of two exponents:

$$\frac{A}{A_0} = e^{-k_{tr}t} + \frac{\beta k_{tr}}{(k_{tr}-k_d)}\left(e^{-k_d t} - e^{-k_{tr}t}\right) \quad (4)$$

In this equation β is the ratio of the specific enzymatic activity of the form N^* (a_{N^*}) to the specific enzymatic activity of the form N (a_N): $\beta \equiv a_{N^*}/a_N$. Solid curve in Fig. 1 was calculated from Eq. (4). The following values of parameters were found: $k_{tr} = 0.065 \pm 0.005$ min^{-1}, $k_d = 0.0067 \pm 0.0006$ min^{-1} and $\beta = 0.73 \pm 0.05$ ($R^2 = 0.9830$). In the frame of scheme (3) the initial stage of thermal inactivation of RMCK is the transition of the enzyme from original native state N to the conformational state N^* with 28%-decrease in the enzymatic activity.

To check the influence of HP-β-CD on thermal inactivation of RMCK, we studied the kinetics of inactivation in the presence of HP-β-CD. The concentration of HP-β-CD was varied in the range of 10–76 mM. The kinetics of inactivation of RMCK was unchanged in the presence of HP-β-CD. As an example, Fig. 1 shows the kinetics of inactivation of RMCK, when 76 mM HP-β-CD was added to the enzyme solution. The data obtained with 76 mM HP-β-CD were analyzed using Eq. (4). The following values of parameters were found: $k_{tr} = 0.056 \pm 0.005$ min^{-1}, $k_d = 0.0057 \pm 0.0006$ min^{-1} and $\beta = 0.67 \pm 0.05$ ($R^2 = 0.9951$). Taking into account the error in calculation of parameters k_{tr}, k_d and β, we can conclude that parameters of RMCK inactivation remain unchanged in the presence of 76 mM HP-β-CD.

3.2. Effect of HP-β-CD on thermal denaturation of RMCK studied by DSC

DSC was used to obtain information on thermostability of RMCK. Curve 1 in Fig. 2 shows the DSC profile for RMCK (0.5 mg mL^{-1}) in 30 mM Hepes–NaOH buffer, pH 8.0, 0.1 M NaCl. The position of maximum of the DSC profile (T_{max}) was found to be 53.7 ± 0.1 °C. When the RMCK concentration was varied in the range 0.25–1 mg mL^{-1}, the shape of the DSC profiles remained unchanged (data not shown). This result agrees with the data obtained in our previous work [26], where thermal denaturation of RMCK was studied in the same buffer, but free of 0.1 M NaCl. These studies demonstrated that the kinetic model of RMCK denaturation does not contain a kinetically significant stage of reversible dissociation of RMCK into monomers.

To check the effect of HP-β-CD on thermostability of RMCK, we compared the DSC profiles obtained in the absence and in the presence of HP-β-CD. The values of T_{max} remained practically constant in the presence of HP-β-CD and were found to be 53.8 ± 0.1, 53.6 ± 0.1 and 53.6 ± 0.1 °C at HP-β-CD concentrations of 15, 38 and 76 mM, respectively. As an example, curve 2 in Fig. 2 shows the DSC profile of RMCK obtained in the presence of 76 mM HP-β-CD. Thus, according to the DSC data HP-β-CD in concentrations up to 76 mM does not affect thermal denaturation of RMCK.

The data on the kinetics of RMCK thermal inactivation showed that a form with higher stability appeared in the course of incubation. Thus, one can expect that the appearance of a more stable fraction of the protein will be registered by DSC as a shift of T_{max} towards the higher temperatures for the preheated samples of RMCK. Actually, we observed the change in the shape of the DSC profiles for the RMCK solutions preincubated for various time intervals at 48 °C. Fig. 3 shows the dependences of C_p^{ex} on temperature for original RMCK (1 mg mL^{-1}, curve 1) and the solutions preincubated at 48 °C for 15, 30, 75 and 140 min (curves 2–5). The reliable estimation of the T_{max} value at high times of incubation presents some difficulties because of the marked diminishing of the amount of the native protein remaining in the solution. However, when calculating the T_{max} value at the incubation times of 15, 30 and 75 min, we observed a well-defined shift of T_{max} towards the higher temperatures. In this series of the DSC experiments the T_{max} value for original RMCK was 53.7 ± 0.1 °C and increased to 54.1 ± 0.1, 54.4 ± 0.1 and 54.6 ± 0.1 °C for RMCK preincubated for 15, 30 and 75 min at 48 °C. These data are indicative of the appearance of the protein fraction more resistant to heating.

The area under curve for the DSC profile (Q_t) may be considered as a measure of the amount of the non-denatured protein. The Q_t value for initial RMCK was found to be 1390 ± 70 kJ mol^{-1}. The inset in Fig. 3 shows the decrease in the Q_t value in the course of incubation of RMCK solution at 48 °C. The dependence of the Q_t value on the preheating time is important in choosing the model of RMCK denaturation. Scheme (3) suggests that the denaturation stage accompanied by the heat absorption is preceded by the conformational transition $N \rightarrow N^*$. If this scheme is valid, the dependence of Q_t on the incubation time should be sigmoid. However, the decrease in

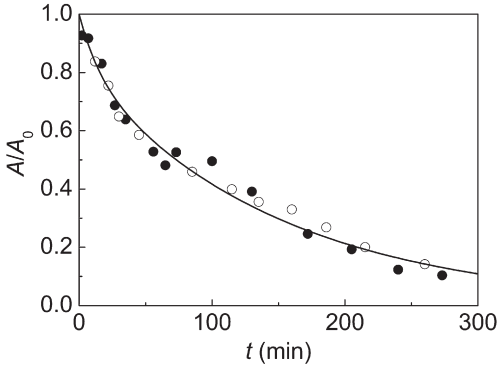

Fig. 1. Dependence of the relative enzymatic activity (A/A_0) of RMCK (0.2 mg mL^{-1}) on time in the absence of HP-β-CD (open circles) and in the presence of 76 mM HP-β-CD (solid circles) at 48 °C (30 mM Hepes–NaOH buffer, pH 8.0, 0.1 M NaCl). A and A_0 are the initial and current enzymatic activity, respectively. Solid curve was calculated from Eq. (4) for the data obtained in the absence of HP-β-CD.

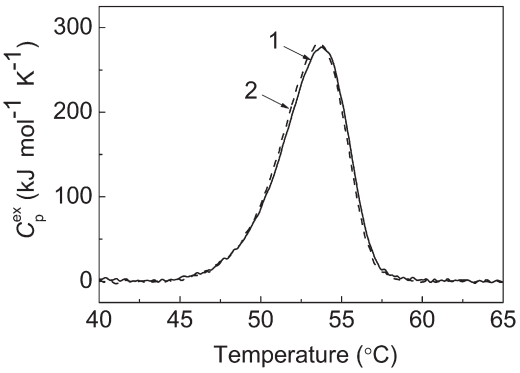

Fig. 2. Thermal denaturation of RMCK studied by DSC. Temperature dependences of the excess heat capacity (C_p^{ex}) of RMCK in the absence of HP-β-CD (1) and in the presence of 76 mM HP-β-CD (2). The initial concentration of RMCK was 1 mg mL^{-1}. Conditions: 30 mM Hepes–NaOH buffer, pH 8.0, 0.1 M NaCl. The heating rate was 1 °C min^{-1}.

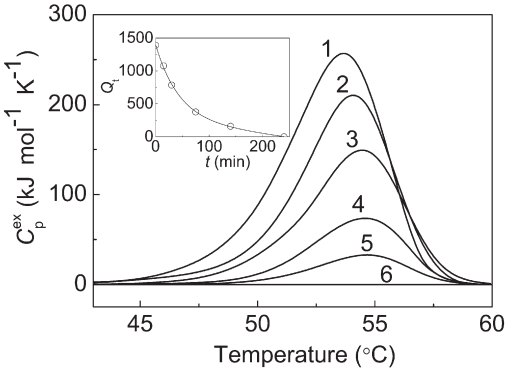

Fig. 3. DSC profiles of RMCK preincubated at 48 °C for the following time intervals: (1) 0, (2) 15, (3) 30, (4) 75, (5) 140 and (6) 240 min. The initial concentration of RMCK was 1 mg mL^{-1}. The heating rate was 1 °C min^{-1}. The inset shows the dependence of the total denaturation heat (Q_t) on the time of incubation of RMCK solution for various time intervals at 48 °C.

the Q_t value in time proceeds without retardation (inset in Fig. 3). This means that scheme (3) is very simplified and should be supplemented by the stage of denaturation of the original form *N*:

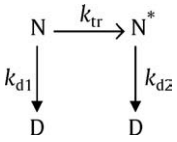

(5)

where k_{d1} and k_{d2} are the denaturation rate constants for unfolding of forms *N* and *N**, respectively. This scheme allows us to describe qualitatively the changes in the shape of the DSC profiles for RMCK preincubated for various time intervals at 48 °C. Attempts to apply scheme (5) to the description of the kinetics of RMCK inactivation were unsuccessful, because this scheme, as applied to the inactivation kinetics, contains four parameters (k_{tr}, k_{d1}, k_{d2}, $\beta \equiv a_{N^*}/a_N$), and reliable estimation of these parameters was impossible.

It should be noted that in our previous work the one-stage model ($N \rightarrow D$) was proposed for thermal denaturation of RMCK [26]. The conclusion regarding the applicability of this model has been made on the basis of the analysis of the DSC profiles obtained at various temperature scanning rates. However, if this model is valid, the shape of the DSC profiles for preheated samples of RMCK would remain unchanged at variation of the incubation time. The change in the position of T_{max} on the DSC profiles (Fig. 3) means that the one-stage model corresponds to a simplified mechanism of RMCK denaturation and cannot be used for adequate description of the kinetics of denaturation.

3.3. Thermal denaturation of RMCK studied by tryptophan fluorescence

The measurements of tryptophan fluorescence of the RMCK solution preheated at 48 °C support the idea that the kinetic model of denaturation involves the formation of the relatively stable intermediate. Fig. 4 demonstrates tryptophan fluorescence spectra of RMCK preincubated at 48 °C for the various time intervals. To remove the aggregated protein, the preheated protein solutions were centrifuged for 30 min at 20,000×*g*. For the original RMCK solution $\lambda_{max} = 332 \pm 1$ nm. When the time of incubation was 15 min, the position of λ_{max} was practically the same ($\lambda_{max} = 333 \pm 1$ nm). The marked shift of λ_{max} at 30– and 75 min incubation ($\lambda_{max} = 346 \pm 1$ and 347 ± 1 nm, respectively) is indicative of the formation of the partially unfolded intermediate with higher degree of exposure of tryptophan residues into medium in comparison with the native molecule.

Thus, as in the case of the DSC profiles for the preheated samples of RMCK, the character of the changes in the tryptophan fluorescence spectra for the RMCK solutions incubated at 48 °C over different time intervals indicates that the simple one-stage model does not agree with the experimental data and the more complex scheme involving the formation of the more stable intermediate (scheme (5)) should be used for the description of the kinetics of RMCK denaturation.

3.4. Effect of HP-β-CD on thermal aggregation of RMCK

To characterize the effect of HP-β-CD on thermal aggregation of RMCK (1 mg mL^{-1}), we studied the accumulation of the aggregated protein in the course of heating at 48 °C. The portion of the aggregated protein (γ_{agg}) was determined by measuring the absorbance of the heated protein solution after centrifugation at 20,000×*g* as described in the section Materials and methods. Fig. 5A shows the dependence of γ_{agg} on time obtained for heating of RMCK in the absence of HP-β-CD (circles). Denaturation of RMCK proceeds as an irreversible process owing to aggregation of the denatured molecules. Therefore we assumed that the portion of the aggregated protein strictly corresponded to the portion of the denatured protein (γ_{den}), and the dependence of γ_{agg} ($\gamma_{agg} = \gamma_{den}$) on time was analyzed in the frame of scheme (5) using Scientist. The following values of parameters were obtained: $k_{tr} = 0.025 \pm 0.005$ min^{-1}, $k_{d1} = 0.031 \pm 0.002$ min^{-1} and $k_{d2} = 0.007 \pm 0.001$ min^{-1} ($R^2 = 0.9460$). Solid curves in Fig. 5 show the theoretical dependences of the concentrations of *N*, *N** and *D* forms on time. Thus, the rates of $N \rightarrow N^*$ transition and denaturation of the form *N* ($N \rightarrow D$) are approximately the same. Denaturation of *N** form proceeds four times slower than denaturation of *N* form.

It is of interest to compare the accumulation of the denatured protein (curve 3 in Fig. 5A) with the diminution of the amount of the native protein expressed by the $(1 - Q_t/Q_{t0})$ value (diamonds in Fig. 5A). If the enthalpy change for the $N \rightarrow N^*$ transition is equal to zero and the heats of unfolding of *N* and *N** forms are identical, the $(1 - Q_t/Q_{t0})$ value should strictly correspond to the portion of the denatured protein. We have assumed that this is true for thermal denaturation of mitochondrial aspartate aminotransferase (mAAT) [49]. Taking into account the errors in the estimation of the total heat denaturation, we may conclude that the above assumptions hold good for RMCK denaturation.

The estimation of the portion of the aggregated protein (γ_{agg}) allows us to characterize the effect of HP-β-CD on thermal aggregation of RMCK. Fig. 5B shows the dependence of the γ_{agg} values on time obtained for RMCK aggregation in the presence of 76 mM HP-β-CD (squares). It can be seen that HP-β-CD suppresses RMCK aggregation.

It is of interest to compare the rates of RMCK inactivation and denaturation. Fig. 6 shows the relationship between the portion of the inactivated protein (γ_{in}) and the portion of the denatured protein

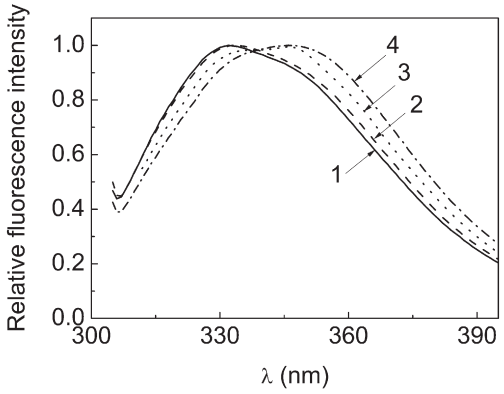

Fig. 4. Tryptophan fluorescence spectra of RMCK preincubated at 48 °C for the following time intervals: (1) 0, (2) 15, (3) 30 and (4) 75 min. The initial concentration of RMCK was 1 mg mL^{-1}. The excitation wavelength was 297 nm.

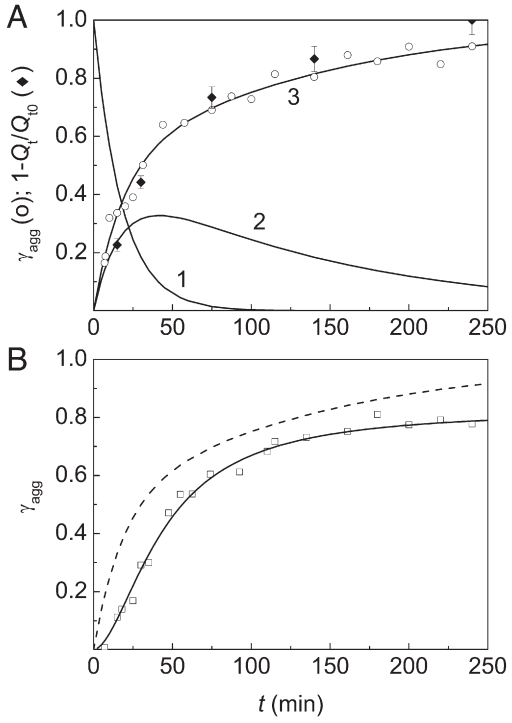

Fig. 5. Effect of HP-β-CD on aggregation of RMCK (1 mg mL^{-1}) at 48 °C. (A). The portion of the aggregated RMCK (γ_{agg}; circles) formed during the incubation of the protein in the absence of HP-β-CD. The points are the experimental data. Each point is the mean of 2–3 measurements. Solid curves 1, 2 and 3 show the changes in the concentrations of *N*, *N** and *D* forms, respectively, in time calculated in accordance with scheme (5) using Scientist. Solid diamonds show the values ($1-Q_t/Q_{t0}$) measured at various intervals of time. (B) The dependence of γ_{agg} (squares) on time for RMCK aggregation in the presence of 76 mM HP-β-CD. A dotted curve shows the dependence of γ_{agg} on time for aggregation of RMCK in the absence of HP-β-CD.

(γ_{den}). It is assumed that $\gamma_{den}=\gamma_{agg}$. To calculate the γ_{in} values, the experimental data on RMCK inactivation (Fig. 1) were approximated by Eq. (4). It is evident that in this procedure Eq. (4) was considered as an empiric expression. As it can be seen from Fig. 6, in the initial stage of RMCK unfolding (at $\gamma_{den}<0.4$) the rate of inactivation is higher than the rate of denaturation. A higher rate of RMCK inactivation is consistent with the idea by Tsou [50,51] that the enzyme active center is more fragile and more easily perturbed than the protein molecule as a whole. Thus, the γ_{in} versus γ_{den} plot may rightly be called the Tsou plot. It should also be noted that we observed such a discrepancy between the inactivation and denaturation rates for mAAT [52].

3.5. Detection of large-sized associates of HP-β-CD by DLS

DLS gives direct evidence for formation of associates in HP-β-CD solutions. Fig. 7 shows the distribution of the particles by size registered in 76 mM solution of HP-β-CD at 48 °C. The peak with $R_h=0.74\pm0.02$ nm corresponds to the monomeric form of HP-β-CD. As can be seen from Fig. 7, two types of associates are observed with the mean values of the hydrodynamic radius of 135 ± 15 and 900 ± 100 nm. The ability of HP-β-CD to self-association agrees with the results of the work by Gonzalez-Gaitano et al. [53], who demonstrated the presence of monomers with $R_h=0.86\pm0.14$ nm and associates with $R_h=62\pm12$ nm in 12 mM solution of HP-β-CD at 25 °C.

3.6. Aggregation of RMCK studied by DLS

Additional information on the mechanism of HP-β-CD action on RMCK aggregation was obtained by DLS. Fig. 8 demonstrates the increment of the light scattering intensity in the course of aggregation of RMCK heated at 48 °C in the absence or in the presence of HP-β-CD.

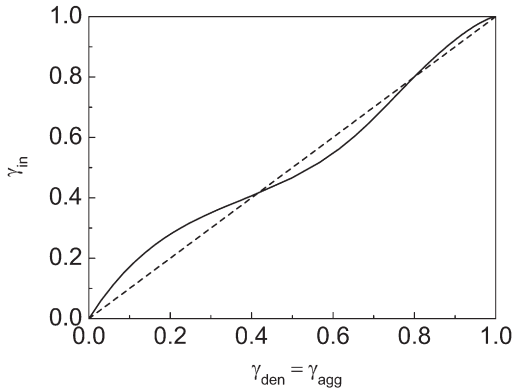

Fig. 6. Relationship between the portion of inactivated RMCK (γ_{in}) and the portion of denatured RMCK (γ_{den}). The γ_{den} value was taken to be equal to the portion of the aggregated RMCK (γ_{agg}). Eq. (4) was used for calculation of the γ_{in} values. The γ_{agg} values were calculated in accordance with scheme (5) using Scientist. The dotted curve corresponds to the case when $\gamma_{in}=\gamma_{den}$.

The addition of HP-β-CD results in the decrease in the increment of the light scattering intensity. As is seen from Fig. 8, there is a lag period on the kinetic curves of RMCK aggregation. To calculate the duration of the lag period (t_0), we used the empiric equation proposed by us earlier [54] (see also [55,56]):

$$I = [K_{LS}(t-t_0)]^2, \quad (6)$$

where I is the light scattering intensity and K_{LS} is a constant with the dimension of (counts/s)^{½} min^{-1} (the lower index LS means "Light Scattering"). It is evident that this equation is used for the analysis of the initial parts of the dependences of the light scattering intensity on time.

Fig. 9 shows the description of the initial parts of the dependences of I on time for thermal aggregation of RMCK using Eq. (2). Fig. 9A corresponds to the kinetic curve obtained in the absence of HP-β-CD, while Fig. 9B demonstrates the kinetic curve obtained in the presence of 38 mM HP-β-CD. The values of parameters t_0 and K_{LS} obtained in this way are given in Table 2. The duration of the lag period (t_0) increases with increasing HP-β-CD concentration. The decrease in the K_{LS} value in the presence of HP-β-CD characterizes the suppression of the aggregation process under the action of HP-β-CD.

DLS allows sizing the protein aggregates formed when RMCK was heated (see Fig. 10). Fig. 10 shows the distribution of particles by size obtained at various times of RMCK incubation at 48 °C in the absence of HP-β-CD (panel A) and in the presence of 76 mM HP-β-CD (panel B). The distribution of particles by size was unimodal, the mean values

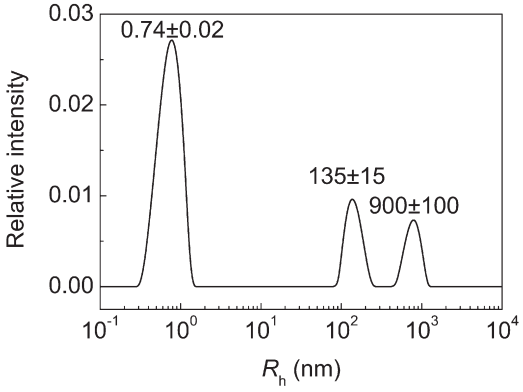

Fig. 7. The distribution of the particles by size registered in the solution of 76 mM HP-β-CD at 48 °C (30 mM Hepes–NaOH buffer, pH 8.0, 0.1 M NaCl).

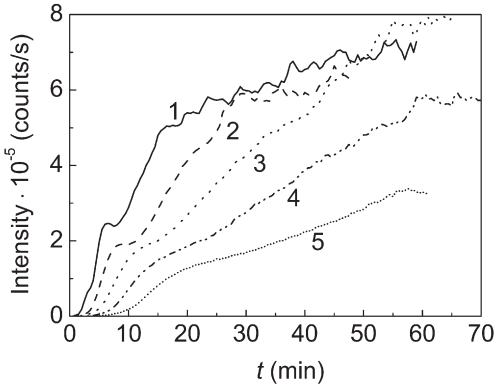

Fig. 8. Dependences of the light scattering intensity on time for thermal aggregation of RMCK (0.2 mg/mL) at 48 °C. The concentrations of HP-β-CD were the following: (1) 0, (2) 8, (3) 38, (4) 61 and (5) 76 mM.

of the hydrodynamic radius of the protein aggregates being shifted towards the higher R_h values with time.

It should be noted that although the HP-β-CD associates are registered in the solution of HP-β-CD, their contribution into the light scattering intensity is negligible in comparison with contribution of the protein aggregates. Therefore the presence of HP-β-CD associates does not interfere with sizing the protein aggregates.

Fig. 11A demonstrates the dependences of the hydrodynamic radius of the protein aggregates on time obtained for aggregation of RMCK in the absence of HP-β-CD (curve 1) or in the presence of HP-β-CD at concentrations of 38 and 76 mM (curves 2 and 3, respectively). Analysis of the initial parts of the dependences of R_h on time shows that they follow the exponential law (see Eq. (2)). As an example, Fig. 11B and C shows the applicability of Eq. (2) to the description of the initial parts of R_h on time obtained in the absence of HP-β-CD (Fig. 11B) and in the presence of 38 mM HP-β-CD (Fig. 11C). With the knowledge of parameter t_0 we can calculate parameters $R_{h,0}$ (the average value of the hydrodynamic radius of the start aggregates)

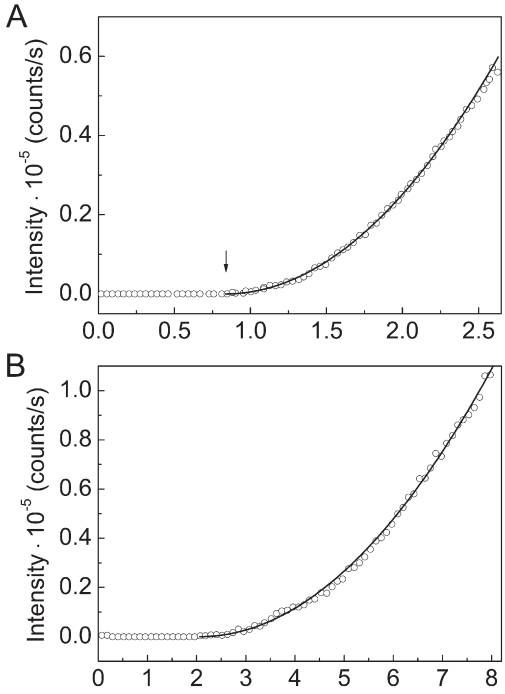

Fig. 9. Initial parts of the dependences of the light scattering intensity on time for thermal aggregation of RMCK at 48 °C. The concentrations of HP-β-CD were the following: (A) 0 and (B) 38 mM. The solid lines were drawn in accordance with Eq. (2). Vertical arrow shows the moment $t = t_0$.

Table 2
Parameters of thermal aggregation of RMCK (0.2 mg mL^{-1}) at 48 °C in the presence of various concentrations of HP-β-CD (30 mM Hepes–NaOH buffer, pH 8.0, 0.1 M NaCl).

[HP-β-CD], mM	t_0, min	K_{LS}, (counts/s)^{½} × min^{-1}	$R_{h,0}$, nm	$1/t_{2R}$, min^{-1}
0	0.84 ± 0.02	136 ± 2	32 ± 2	0.81 ± 0.03
8	1.05 ± 0.04	66 ± 2	46 ± 1	0.40 ± 0.01
15	1.39 ± 0.03	83 ± 2	58 ± 5	0.37 ± 0.03
31	2.07 ± 0.02	62 ± 1	82 ± 5	0.24 ± 0.02
38	2.07 ± 0.02	56 ± 1	74 ± 4	0.28 ± 0.02
46	2.41 ± 0.03	47 ± 1	89 ± 4	0.20 ± 0.01
61	2.44 ± 0.05	33 ± 1	129 ± 7	0.102 ± 0.015
76	2.69 ± 0.05	14 ± 1	138 ± 6	0.081 ± 0.007

and t_{2R} (the time interval over which the R_h value is doubled). These parameters are given in Table 2. As it can be seen, the hydrodynamic radius of the start aggregates increases with increasing HP-β-CD concentration from $R_{h,0} = 32 \pm 2$ nm measured at [HP-β-CD] = 0 to 138 ± 6 nm measured at [HP-β-CD] = 76 mM. The 10-fold decrease in the $1/t_{2R}$ value is observed in the presence of 76 mM HP-β-CD in comparison with the control ([HP-β-CD] = 0). The diminution of the $1/t_{2R}$ value characterizes the suppression of the rate of RMCK aggregation under the action of HP-β-CD.

It is of interest to compare parameter K_{LS}, characterizing the aggregation rate estimated on the basis of the measurements of the light scattering intensity increment, on the one hand, and the reciprocal value of parameter t_{2R}, characterizing the aggregation rate estimated on the basis of the measurements of the increase in the size of the protein aggregates, on the other hand. There is a good correlation between K_{LS} and $1/t_{2\,R}$ values ($R^2 = 0.859$) (see Fig. 12).

Fig. 13 shows the dependence of the relative rate of RMCK aggregation expressed as $K_{LS}/(K_{LS})_0$ or $(1/t_{2R})/(1/t_{2R})_0$ on the concentration of HP-β-CD. $(K_{LS})_0$ and $(1/t_{2R})_0$ are the values of the corresponding parameters at [HP-β-CD] = 0. As can be seen from this figure, 40%-decrease in the aggregation rate occurred in the interval of HP-β-CD concentrations from 0 to 4 mM. The further

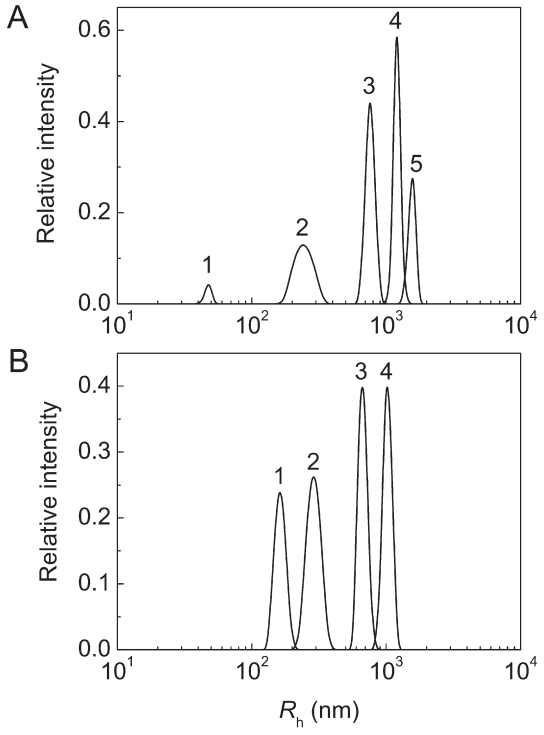

Fig. 10. Thermal aggregation of RMCK (0.2 mg mL^{-1}) registered by DLS at 48 °C in the absence of HP-β-CD (A) and in the presence of 76 mM of HP-β-CD (B). Distributions of particles by size were obtained at the following times of incubation: panel A (1) 1.5, (2) 5, (3) 20, (4) 40 and (5) 60 min; panel B (1) 5, (2) 20, (3) 40 and (4) 60 min.

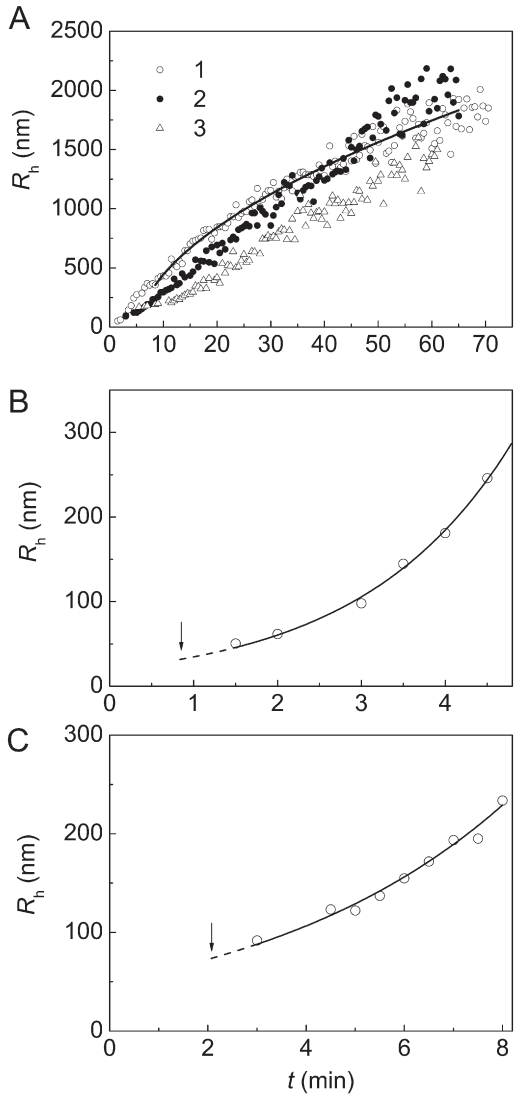

Fig. 11. Dependences of the hydrodynamic radius (R_h) of the protein aggregates on time for RMCK aggregation at 48 °C. (A) The full dependences of R_h on time obtained in the presence of various HP-β-CD concentrations: (1) 0, (2) 38 and (3) 76 mM. The solid curve was calculated from Eq. (1). The initial parts of the dependences of R_h on time obtained in the absence of HP-β-CD (B) and in the presence of 38 mM of HP-β-CD (C). The points represent experimental data. The solid curves were drawn in accordance with Eq. (2). Vertical arrows show the moment $t = t_0$.

increase in HP-β-CD concentration from 4 to 76 mM was accompanied by the linear decrease in the aggregation rate. Such a character of the dependence of the aggregation rate on the HP-β-CD concentration may be explained as follows. One can expect that the side chains of aromatic amino acids with the high degree of exposure in the unfolded protein bind HP-β-CD with higher affinity and give the highest contribution to the rate of RMCK aggregation. As for the residues of aromatic amino acids with the low degree of exposure, they reveal the relatively low affinity to HP-β-CD and give the low contribution to the rate of RMCK aggregation.

The fact that the dependence of the hydrodynamic radius of the protein aggregates on time follows the exponential law is indicative of the fulfillment of the RLCA regime for the aggregation process. The theory predicts that the transition of the RLCA regime to the DLCA regime should occur as the size of aggregates increases [40]. The reason is that the increase in the size of an aggregate results in the increase of the contact region of the colliding particles and, consequently, in the enhancement of the sticking probability. When the DLCA regime is fulfilled, the dependence of the hydrodynamic

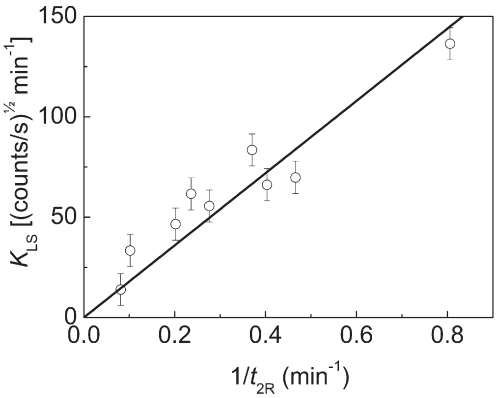

Fig. 12. Correlation between parameter K_{LS} calculated from the dependences of the light scattering intensity on time and parameter $1/t_{2R}$ calculated from the dependences of R_h on time for RMCK aggregation at 48 °C.

radius of the protein aggregates on time should follow the power law (see Eq. (1)). Analysis of the dependence of R_h on time for RMCK aggregation registered in the absence of HP-β-CD shows that at rather high values of time (t>10 min) this dependence is satisfactorily described by Eq. (1). The value of the fractal dimension (d_f) of the protein aggregates was found to be 1.81 ± 0.02.

Suppression of thermal aggregation of RMCK by HP-β-CD is consistent with the results of the studies where the protective action of cyclodextrins was demonstrated for thermal aggregation of citrate synthase, horse liver alcohol dehydrogenase, mink and porcine growth hormones and α-amylase [15–18,57]. The approaches elaborated in the present work allow us to obtain the quantitative characteristics of the anti-aggregating activity of HP-β-CD. These characteristics include the duration of lag period (t_0) and the rate of aggregation expressed by parameters K_{LS} and $1/t_{2R}$. The correlation between parameters K_{LS} and $1/t_{2R}$ has been demonstrated in the present work. This means that even a simple measurement of the light scattering intensity of the protein solutions makes it possible to quantitatively estimate the protein aggregation rate.

4. Conclusions

According to the results of the present work, thermal denaturation of RMCK proceeds as a two-stage process. The reliability theory gives the methodological basis for analysis of the failures in biological systems [58–60]. The failure rate as a function of time for living organisms, as in the case of technical devices, looks to take the "bathtube curve" [61]. Initially, the failure rate is high and decreases

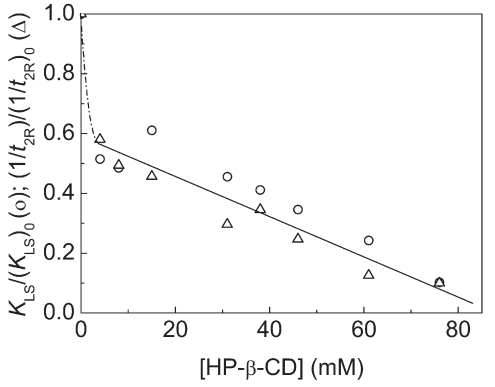

Fig. 13. The dependence of the relative rate of thermal aggregation of RMCK (0.2 mg mL^{-1}) expressed as $K_{LS}/(K_{LS})_0$ (circles) and $(1/t_{2R})/(1/t_{2R})_0$ (triangles) on the concentration of HP-β-CD at 48 °C. $(K_{LS})_0$ and $(1/t_{2R})_0$ are the values of the corresponding parameters at [HP-β-CD] = 0.

with time. The initial part of the dependence of the failure rate on time may be considered as the period of "burning-out" of defective components [61]. The initial fast stage of RMCK denaturation may be connected with adaptation of the protein molecule to the high temperatures and the transition of the protein from metastable state (N) to more stable state (N^*) remaining the catalytic activity. The elevation of temperature favors overcoming the activation barrier between these states. The metastable states of the proteins have been discussed in detail by Popov et al. [62].

It is of interest to compare the efficiency of suppression of protein aggregation by chaperones and cyclodextrins. When studying the anti-aggregating ability of α-crystallin, one of the small heat shock proteins, we showed that suppression of protein aggregation may be characterized by the increase in the duration of the lag period (t_0) on the kinetic curves of aggregation and the decrease in the aggregation rate expressed as parameter $1/t_{2R}$. Simultaneously we observed a sharp decrease in the size of the primary clusters registered in the system at the moment when the light scattering intensity began to increase [34,35,44–47].

In the case of suppression of protein aggregation by cyclodextrins, as illustrated by the kinetics of RMCK aggregation in the presence of HP-β-CD, we also observed the increase in parameter t_0 and the decrease in parameter $1/t_{2R}$. It is evident that when studying the anti-aggregating ability of a low-molecular weight "chaperone" (cyclodextrin), we should use substantially higher molar concentrations than in the case of the chaperone of protein nature. There is an appreciable distinction between the mechanisms of suppression of protein aggregation by chaperones and cyclodextrins. In contrast to the chaperones of a protein nature, cyclodextrins provoke an increase in the size of the start aggregates.

Acknowledgements

This study was funded by the Russian Foundation for Basic Research (grant 08-04-00666-a) and the Program "Molecular and Cell Biology" of the Presidium of the Russian Academy of Sciences.

References

[1] J. Szejtli, Introduction and general overview of cyclodextrin chemistry, Chem. Rev. 98 (1998) 1743–1754.
[2] B. Hingerty, B. Klar, G.L. Hardgrove, C. Betzel, W. Saenger, Neutron diffraction of alpha, beta and gamma cyclodextrins: hydrogen bonding patterns, J. Biomol. Struct. Dyn. 2 (1984) 249–260.
[3] K. Uekama, F. Hirayama, T. Irie, Cyclodextrin drug carrier systems, Chem. Rev. 98 (1998) 2045–2076.
[4] T. Loftsson, M.E. Brewster, Pharmaceutical applications of cyclodextrins. 1. Drug solubilization and stabilization, J. Pharm. Sci. 85 (1996) 1017–1025.
[5] F. Hapiot, S. Tilloy, E. Monflier, Cyclodextrins as supramolecular hosts for organometallic complexes, Chem. Rev. 106 (2006) 767–781.
[6] K.A. Connors, Population characteristics of cyclodextrin complex stabilities in aqueous solution, J. Pharm. Sci. 84 (1995) 843–888.
[7] M.V. Rekharsky, Y. Inoue, Complexation thermodynamics of cyclodextrins, Chem. Rev. 98 (1998) 1875–1918.
[8] M.E. Brewster, M.S. Hora, J.W. Simpkins, N. Bodor, Use of 2-hydroxypropyl-beta-cyclodextrin as a solubilizing and stabilizing excipient for protein drugs, Pharm. Res. 8 (1991) 792–795.
[9] F. Hirayama, K. Uekama, Cyclodextrin-based controlled drug release system, Adv. Drug Deliv. Rev. 36 (1999) 125–141.
[10] A. Cooper, Effect of cyclodextrins on the thermal stability of globular proteins, J. Am. Chem. Soc. 114 (1992) 9208–9209.
[11] T. Yamamoto, N. Fukui, A. Hori, Y. Matsui, Circular dichroism and fluorescence spectroscopy studies of the effect of cyclodextrins on the thermal stability of chicken egg white lysozyme in aqueous solution, J. Mol. Struct. 782 (2006) 60–66.
[12] K. Yoshikiyo, R. Takeshita, T. Yamamoto, T. Takahashi, Y. Matsui, The effects of cyclodextrins on the thermal denaturation and renaturation processes of bovine pancreatic ribonuclease A in an aqueous solution studied by circular dichroism and fluorescence spectroscopy, J. Mol. Struct. 832 (2007) 96–100.
[13] O.I. Maloletkina, K.A. Markosyan, R.A. Asriyants, V.N. Orlov, B.I. Kurganov, Antichaperone activity of cyclodextrin derivatives, Dokl. Biochem. Biophys. 427 (2009) 199–201 (Mosc).
[14] A. Barzegar, A.A. Moosavi-Movahedi, S. Rezaei-Zarchi, A.A. Saboury, M.R. Ganjali, P. Norouzi, G.H. Hakimelahi, F.Y. Tsai, The mechanisms underlying the effect of alpha-cyclodextrin on the aggregation and stability of alcohol dehydrogenase, Biotechnol. Appl. Biochem. 49 (2008) 203–211.
[15] S.I. Soares, R.M. Goncalves, I. Fernandes, N. Mateus, V. de Freitas, Mechanistic approach by which polysaccharides inhibit alpha-amylase/procyanidin aggregation, J. Agric. Food Chem. 57 (2009) 4352–4358.
[16] M. Toda, H. Itoh, Y. Kondo, F. Hamada, HSP90-like artificial chaperone activity based on indole beta-cyclodextrin, Bioorg. Med. Chem. 15 (2007) 1983–1988.
[17] J.F. Sigurjonsdottir, T. Loftsson, M. Masson, Influence of cyclodextrins on the stability of the peptide salmon calcitonin in aqueous solution, Int. J. Pharm. 186 (1999) 205–213.
[18] H.S. Samra, F. He, A. Bhambhani, J.D. Pipkin, R. Zimmerer, S.B. Joshi, C.R. Middaugh, The effects of substituted cyclodextrins on the colloidal and conformational stability of selected proteins, J. Pharm. Sci. (2010), doi:10.1002/jps.22053.
[19] M.S. Wang, S. Boddapati, M.R. Sierks, Cyclodextrins promote protein aggregation posing risks for therapeutic applications, Biochem. Biophys. Res. Commun. 386 (2009) 526–531.
[20] S. Putney, W. Herlihy, N. Royal, H. Pang, H.V. Aposhian, L. Pickering, R. Belagaje, K. Biemann, D. Page, S. Kuby, P. Schimmel, Rabbit muscle creatine phosphokinase. CDNA cloning, primary structure and detection of human homologues, J. Biol. Chem. 259 (1984) 14317–14320.
[21] J.K. Rao, G. Bujacz, A. Wlodawer, Crystal structure of rabbit muscle creatine kinase, FEBS Lett. 439 (1998) 133–137.
[22] T.J. Zhao, S. Feng, Y.L. Wang, Y. Liu, X.C. Luo, H.M. Zhou, Y.B. Yan, Impact of intra-subunit domain–domain interactions on creatine kinase activity and stability, FEBS Lett. 580 (2006) 3835–3840.
[23] H.W. He, J. Zhang, H.M. Zhou, Y.B. Yan, Conformational change in the C-terminal domain is responsible for the initiation of creatine kinase thermal aggregation, Biophys. J. 89 (2005) 2650–2658.
[24] F. Couthon, E. Clottes, C. Vial, Refolding of SDS- and thermally denatured MM-creatine kinase using cyclodextrins, Biochem. Biophys. Res. Commun. 227 (1996) 854–860.
[25] J.H. Bai, S.Y. Zheng, H.M. Zhou, Inactivation of creatine kinase is due to the conformational changes of the active sites during thermal denaturation, Biochem. Mol. Biol. Int. 45 (1998) 941–951.
[26] A.E. Lyubarev, B.I. Kurganov, V.N. Orlov, H.M. Zhou, Two-state irreversible thermal denaturation of muscle creatine kinase, Biophys. Chem. 79 (1999) 199–204.
[27] J.M. Cox, C.A. Davis, C. Chan, M.J. Jourden, A.D. Jorjorian, M.J. Brym, M.J. Snider, C.L. Borders Jr., P.L. Edmiston, Generation of an active monomer of rabbit muscle creatine kinase by site-directed mutagenesis: the effect of quaternary structure on catalysis and stability, Biochemistry 42 (2003) 1863–1871.
[28] F.G. Meng, Y.K. Hong, H.W. He, A.E. Lyubarev, B.I. Kurganov, Y.B. Yan, H.M. Zhou, Osmophobic effect of glycerol on irreversible thermal denaturation of rabbit creatine kinase, Biophys. J. 87 (2004) 2247–2254.
[29] T.J. Zhao, Y. Liu, Z. Chen, Y.B. Yan, H.M. Zhou, The evolution from asparagine or threonine to cysteine in position 146 contributes to generation of a more efficient and stable form of muscle creatine kinase in higher vertebrates, Int. J. Biochem. Cell Biol. 38 (2006) 1614–1623.
[30] D.M. Dawson, H.M. Eppenberger, N.O. Kaplan, The comparative enzymology of creatine kinases. II. Physical and chemical properties, J. Biol. Chem. 242 (1967) 210–217.
[31] L. Noda, S.A. Kuby, H. Lardy, ATP-creatine transphosphorylase, Meth. Enzymol. 2 (1955) 11505–11610.
[32] P.H. Stothart, Determination of partial specific volume and absolute concentration by densimetry, Biochem. J. 219 (1984) 1049–1052.
[33] L.V. Belousova, S.N. Fedosov, E.L. Moskvitina, L.P. Grinio, V.S. Rafanov, Potentiometric method for determining serum creatine kinase activity, Vopr. Med. Khim. 33 (1987) 138–140 Russian.
[34] H.A. Khanova, K.A. Markossian, B.I. Kurganov, A.M. Samoilov, S.Y. Kleimenov, D.I. Levitsky, I.K. Yudin, A.C. Timofeeva, K.O. Muranov, M.A. Ostrovsky, Mechanism of chaperone-like activity. Suppression of thermal aggregation of betaL-crystallin by alpha-crystallin, Biochemistry 44 (2005) 15480–15487.
[35] H.A. Khanova, K.A. Markossian, S.Y. Kleimenov, D.I. Levitsky, N.A. Chebotareva, N. V. Golub, R.A. Asryants, V.I. Muronetz, L. Saso, I.K. Yudin, K.O. Muranov, M.A. Ostrovsky, B.I. Kurganov, Effect of alpha-crystallin on thermal denaturation and aggregation of rabbit muscle glyceraldehyde-3-phosphate dehydrogenase, Biophys. Chem. 125 (2007) 521–531.
[36] A.V. Meremyanin, T.B. Eronina, N.A. Chebotareva, S.Y. Kleimenov, I.K. Yudin, K.O. Muranov, M.A. Ostrovsky, B.I. Kurganov, Effect of alpha-crystallin on thermal aggregation of glycogen phosphorylase *b* from rabbit skeletal muscle, Biochemistry 72 (2007) 518–528 (Mosc).
[37] N. Golub, A. Meremyanin, K. Markossian, T. Eronina, N. Chebotareva, R. Asryants, V. Muronets, B. Kurganov, Evidence for the formation of start aggregates as an initial stage of protein aggregation, FEBS Lett. 581 (2007) 4223–4227.
[38] K.A. Markossian, H.A. Khanova, S.Y. Kleimenov, D.I. Levitsky, N.A. Chebotareva, R. A. Asryants, V.I. Muronetz, L. Saso, I.K. Yudin, B.I. Kurganov, Mechanism of thermal aggregation of rabbit muscle glyceraldehyde-3-phosphate dehydrogenase, Biochemistry 45 (2006) 13375–13384.
[39] D.A. Weitz, J.S. Huang, M.Y. Lin, J. Sung, Limits of the fractal dimension for irreversible kinetic aggregation of gold colloids, Phys. Rev. Lett. 54 (1985) 1416–1419.
[40] D.A. Weitz, M.Y. Lin, Dynamic scaling of cluster–mass distributions in kinetic colloid aggregation, Phys. Rev. Lett. 57 (1986) 2037–2040.
[41] K.A. Markossian, N.V. Golub, H.A. Khanova, D.I. Levitsky, N.B. Poliansky, K.O. Muranov, B.I. Kurganov, Mechanism of thermal aggregation of yeast alcohol dehydrogenase I Role of intramolecular chaperone, Biochim. Biophys. Acta 1784 (2008) 1286–1293.
[42] K.A. Markossian, B.I. Kurganov, D.I. Levitsky, H.A. Khanova, N.A. Chebotareva, A.M. Samoilov, T.B. Eronina, N.V. Fedurkina, L.G. Mitskevich, A.V. Merem'yanin, S.Y.

Kleymenov, V.F. Makeeva, V.I. Muronets, I.N. Naletova, I.N. Shalova, R.A. Asryants, E.V. Schmalhausen, L. Saso, Y.V. Panyukov, E.N. Dobrov, I.K. Yudin, K.O. Muranov, A.C. Timofeeva, M.A. Ostrovsky, Mechanisms of chaperone-like activity, in: T.R. Obalinsky (Ed.), Protein Folding: New Research, Nova Science Publishers Inc., NY, 2006, pp. 89–171.

[43] A.V. Meremyanin, T.B. Eronina, N.A. Chebotareva, B.I. Kurganov, Kinetics of thermal aggregation of glycogen phosphorylase *b* from rabbit skeletal muscle. Mechanism of protective action of alpha-crystallin, Biopolymers 89 (2008) 124–134.

[44] N.V. Golub, K.A. Markossian, M.V. Sholukh, K.O. Muranov, B.I. Kurganov, Study of kinetics of thermal aggregation of mitochondrial aspartate aminotransferase by dynamic light scattering: protective effect of alpha-crystallin, Eur. Biophys. J. 38 (2009) 547–556.

[45] K.A. Markossian, N.V. Golub, S.Y. Kleymenov, K.O. Muranov, M.V. Sholukh, B.I. Kurganov, Effect of α-crystallin on thermostability of mitochondrial aspartate aminotransferase, Int. J. Biol. Macromol. 44 (2009) 441–446.

[46] K.A. Markossian, I.K. Yudin, B.I. Kurganov, Mechanism of suppression of protein aggregation by alpha-crystallin, Intern. J. Mol. Sci. 10 (2009) 1314–1345.

[47] K.A. Markossian, N.V. Golub, N.A. Chebotareva, R.A. Asryants, I.N. Naletova, V.I. Muronetz, K.A. Muranov, B.I. Kurganov, Comparative analysis of the effects of alpha-crystallin and GroEL on the kinetics of thermal aggregation of rabbit muscle glyceraldehyde-3-phosphate dehydrogenase, Protein J. 29 (2010) 11–25.

[48] Scientist for Experimental Data Fitting, Microsoft Windows Version 2.0, Micro-Math, Inc, Salt Lake City, 1995.

[49] N.V. Golub, K.A. Markossian, N.V. Kasilovich, M.V. Sholukh, V.N. Orlov, B.I. Kurganov, Thermal inactivation, denaturation and aggregation of mitochondrial aspartate aminotransferase, Biophys. Chem. 135 (2008) 125–131.

[50] C.L. Tsou, Conformational flexibility of enzyme active sites, Science 262 (1993) 380–381.

[51] C.L. Tsou, Active site flexibility in enzyme catalysis, Ann. NY Acad. Sci. 864 (1998) 1–8.

[52] N.V. Golub, K.A. Markosyan, M.V. Sholukh, N.V. Kasilovich, S.Y. Kleimenov, D.I. Levitskii, B.I. Kurganov, Heat-induced inactivation and denaturation of mitochondrial aspartate aminotransferase, Dokl. Biochem. Biophys. 415 (2007) 203–205 (Mosc).

[53] G. Gonzalez-Gaitano, P. Rodriguez, J.R. Isasi, M. Fuentes, G. Tardajos, M. Sanchez, The aggregation of cyclodextrins as studied by photon correlation spectroscopy, J. Incl. Phenom. Macrocycl. Chem. 44 (2002) 101–105.

[54] B.I. Kurganov, Kinetics of heat aggregation of proteins, Biochemistry 63 (1998) 364–366 (Mosc).

[55] T.B. Eronina, N.A. Chebotareva, S.G. Bazhina, V.F. Makeeva, S.Y. Kleymenov, B.I. Kurganov, Effect of proline on thermal inactivation, denaturation and aggregation of glycogen phosphorylase *b* from rabbit skeletal muscle, Biophys. Chem. 141 (2009) 66–74.

[56] Z.M. Bumagina, B.Y. Gurvits, N.A. Artemova, K.O. Muranov, I.K. Yudin, B.I. Kurganov, Mechanism of suppression of dithiothreitol-induced aggregation of bovine alpha-lactalbumin by alpha-crystallin, Biophys. Chem. 146 (2010) 108–117.

[57] E. Bajorunaite, A. Cirkovas, K. Radzevicius, K.L. Larsen, J. Sereikaite, V.A. Bumelis, Anti-aggregatory effect of cyclodextrins in the refolding process of recombinant growth hormones from *Escherichia coli* inclusion bodies, Int. J. Biol. Macromol. 44 (2009) 428–434.

[58] I.V. Berezin, S.D. Varfolomeev, Biokinetics, Nauka, Moscow, 1979 Russian.

[59] B.M. Ayyub, R.H. McCuen (Eds.), Probability, Statistics, Reliability for Engineers and Scientists, Chapman and Hall/CRC, Boca Raton, FL, 2003.

[60] M. Rausand, A. Hoyland (Eds.), System Reliability Theory: Models, Statistical Methods, and Applications, Wiley-Interscience, Hoboken, New York, 2003.

[61] L.A. Gavrilov, N.S. Gavrilova, Reliability theory of aging and longevity, in: E.J. Masoro, S.N. Austad (Eds.), Handbook of the Biology of Aging, Academic Press, San Diego, CA, USA, 2006, pp. 3–42.

[62] E.M. Popov, V.V. Demin, E.D. Shibanova, Problem of the Protein. Spatial Structure of the Protein, v. 2, Nauka, Moscow, 1996, pp. 348–356, Russian.